2025 47th Annual International Conference of the IEEE Engineering in Medicine and Biology Society (EMBC) | 979-8-3315-8618-8/25/$31.00 ©2025 Authors | DOI: 10.1109/EMBC58623.2025.11253272

Network-Level Characterization of Hippocampal Disruptions in Alzheimer's Disease Using Large-Scale Electrophysiology

Brett Addison Emery, Shahrukh Khanzada, Xin Hu, Maria Anna Maggi, Silvia Bisti, and Hayder Amin*, *Member, IEEE*

***Abstract*—Alzheimer's disease (AD), a progressive neurodegenerative disorder, is projected to affect over 130 million people globally by 2050. While extensive efforts have focused on targeting molecular hallmarks such as amyloid-beta (Aβ) plaques and tau pathology, network-level dysfunction remains a critical but underexplored component of AD progression. Disruptions in hippocampal-cortical (HC) circuit activity emerge early in AD, compromising memory processing and cognitive functions. Characterizing these disruptions requires high-resolution platforms capable of capturing network-wide spatiotemporal dynamics. To address this, we implemented a high-density microelectrode array (HD-MEA) biosensor to assess large-scale electrophysiological activity in ex vivo hippocampal slices from well-established APP^{NL} and APP^{NL-G-F} mouse models. Our approach quantifies hippocampal oscillatory disturbances and examines their modulation by saffron, a natural compound with reported neuroprotective properties. Results indicate that hippocampal network activity is progressively impaired in APP^{NL-G-F} mice, particularly in sharp-wave ripple (SWR) and multi-unit activity (MUA) patterns. The HD-MEA platform provides a scalable tool for investigating AD-associated network dysfunctions and exploring potential modulatory interventions.**

I. Introduction

Network-level organizing principles rely on the dynamic organization of neural assemblies, which form stable structures for information encoding and processing, through synchronized firing patterns and coordinated activity. This coordination allows for the transmission of signals across brain regions and facilitates the integration of sensory input and memory processes [1], [2], [3]. In Alzheimer's disease (AD), early disruptions in hippocampal-cortical (HC) circuits impair these coordinated processes, leading to progressive cognitive decline [4], [5], [6]. While molecular and cellular alterations such as Aβ aggregation and tau pathology have been extensively studied, the network-level consequences of these changes remain less understood [7], [8]. Characterizing network dysfunction in AD is essential for identifying functional biomarkers and potential intervention points. In particular, changes in oscillatory dynamics—from slow delta and theta waves to high-frequency gamma rhythms and sharp-wave ripples (SWRs)—provide valuable insight into the integrity of hippocampal circuits. Given the sensitivity of SWRs to excitatory-inhibitory (E/I) balance and synaptic integrity, their disruption serves as a key marker of neurodegenerative progression [1], [2], [3]. However, studying these patterns requires advanced electrophysiological platforms capable of capturing large-scale network activity with high spatiotemporal resolution. To investigate the modulation of HC dynamics and oscillatory patterns in AD, we employed a large-scale, brain-on-chip biosensing platform based on a high-density, CMOS-based microelectrode array (HD-MEA) [9], [10], [11], [12].

With our HD-MEA platform, we characterize HC network disruptions in two well-established AD mouse models, APP^{NL} and APP^{NL-G-F}[13], [14]. Additionally, we examine the effects of saffron, a natural compound with reported neuroprotective properties, on modulating circuit activity. Saffron was chosen because of its demonstrated antioxidative, anti-inflammatory, and neuroprotective effects, which contribute to synaptic maintenance and cognitive enhancement in preclinical models [12], [15], [16]. Unlike single-target pharmacological agents, saffron provides a multi-faceted approach that aligns with the complex pathology of AD. This makes it particularly suitable for studying network-wide disruptions and potential circuit restoration in AD models.

II. Materials and Methods

A. CMOS-based Biosensor

Large-scale HC recordings were performed using HD-MEA and a biosignal sensing platform (3Brain AG, Switzerland) customized to our recording setups (Fig. 1, a and b). Biosensor HD-MEA chips contain 4096 recording electrodes with a 42-µm pitch size to compose an active sensing area of ~7 mm^2, sufficient to record the entire HC circuit. Recordings were band-pass filtered from 1Hz to 5 kHz, ensuring the capture of local field potentials (LFPs), SWRs, and multi-unit activity (MUA) across a broad frequency spectrum.

B. Acute Hippocampal Slice Preparation

All work and animal procedures were performed in accordance with European and national regulations (Tierschutzgesetz) and were approved by the local authority (Landesdirektion Sachsen; 25–5131/476/14). Acute, horizontal 300 µm thick hippocampal-cortical slices were obtained from 36-week-old APP^{NL} and APP^{NL-G-F} female mice and prepared according to our previously published studies [9], [10], [11]. Slices were sectioned at 0–2 °C in a high sucrose perfusate solution (pH = 7.25–7.35; 345–355 mOsm/L) saturated with 95% O_2 and 5% CO_2 and containing

Research supported from basic institutional funds (DZNE) and the ERANET-NEURON (ResiPreS).

B.A. Emery, S. Khanzada, X. Hu, and H. Amin are with the Biohybrid Neuroelectronics Laboratory (BIONICS) at the German Center for Neurodegenerative Diseases (DZNE), Tatzberg 41, 01307 Dresden, Germany *Corresponding author (Tel: +49351210463602 - E-mail hayder.amin@dzne.de).

M. A. Maggi is with Hortus Novus, Canistro, 67051 L'Aquila, Italy.

S. Bisti is with the National Institute of Biostructure and Biosystem (INBB), V. le Medaglie D'Oro 305, 00136 Roma, Italy.

in mM: 250 Sucrose, 10 Glucose, 1.25 NaH_2PO_4, 24 $NaHCO_3$, 2.5 KCl, 0.5 Ascorbic acid, 4 $MgCl_2$, 1.2 $MgSO_4$, 0.5 $CaCl_2$. Slices were incubated at 32°C for 45 minutes and recovered at room temperature for one hour in a recording perfusate solution (pH = 7.25–7.35; 305–315 mOsm/L) saturated with 95% O_2 and 5% CO_2 and containing in mM: 127 NaCl, 3.5 KCl, 1.25 NaH_2PO_4, 26 $NaHCO_3$, 10 Glucose, 1 $MgSO_4$, 2.5 $CaCl_2$.

C. Biochemically-Modulated Hippocampal Recordings

Slices were placed and coupled onto the HD-MEA chip using a custom-made platinum harp placed on the tissue. A heat-stabilized perfusion system (ALA Scientific Instruments, USA) was integrated to deliver oxygenated recording perfusate to the brain-on-chip interface at a flow rate of 4.5 mL/min and was temperature-controlled at 37 °C throughout the experiment. The first extracellular recording for APP^{NL} and APP^{NL-G-F} captured the baseline spontaneous circuit activation induced by 100 µM 4AP (Sigma-Aldrich, Germany) without saffron (0 µg/mL). Following this, incremental concentrations of saffron (25, 50, and 75 µg/mL) were successively added to the perfusate containing 100 µM 4AP, and ten minutes of extracellular recordings were collected for each concentration [12]. Stigmas of saffron derived from (Hortus Novus srl, Italy) were prepared as a stock of 1 mg/mL in double distilled water prior to the experiment [12], [15], [16]. To obtain the spatial arrangement of tissue relative to extracellular recordings during offline analysis, an optical imaging microscope was incorporated with the HD-MEA biosignal sensing platform to capture HC brain slice structures following recordings.

D. Large-Scale, Network-Wide Analyses

To spatially characterize circuit functionality, active electrodes were grouped offline into specific layers based on molecular structural information from the corresponding slice image. HC subregional layers included DG, hilus, CA3, CA1, entorhinal cortex (EC), and perirhinal cortex (PC). LFP event and MUA detection was performed using hard thresholding and PTSD algorithms in commercially available software (3Brain AG), while SWR event detection was performed as previously described [10]. Detected events were band-pass filtered for LFPs (1-100 Hz), SWRs (120-240 Hz), and MUA (300-1000 Hz) patterns and preprocessed using an adaptive waveform-based thresholding platform - DENOISING – to remove artifacts and assign timestamps [17]. All further analyses were developed as custom-written Python scripts.

Event-based parameters including - active channel count, mean event rate, and event duration were selected to describe network and oscillatory pattern dynamics. To compare regional activation and temporal event distribution across HD-MEA electrodes between two concentrations, raster plots were generated from consecutive phase recordings. To examine specific temporal signal traces, supervised waveform thresholding algorithms extracted exemplified regional LFP, SWR, and MUA signal traces. To determine the power distribution and dominant frequency of each oscillatory pattern a frequency-time dynamic in pseudo-color spectrograms was constructed for a selected time window. Finally, all statistical analyses were performed with Originlab 2024. Differences between groups were examined for statistical significance using one-way analysis of variance (ANOVA) followed by Tukey's posthoc testing. $p < 0.05$ was considered significant.

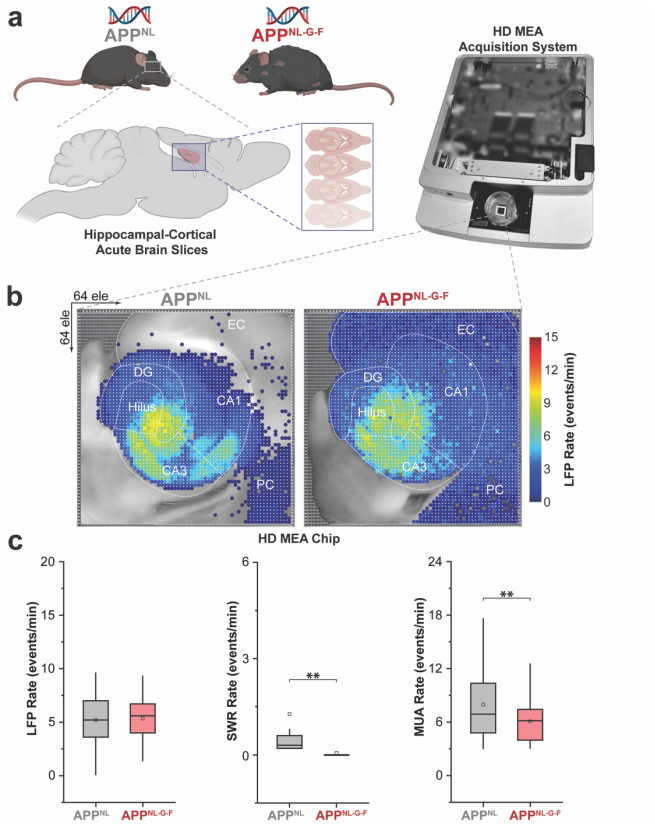

Figure 1: Schematic overview of experimental paradigm and HD-MEA biosensing platform (a) implemented for recording large-scale activation of HC slices-on-chip. APP^{NL} and APP^{NL-G-F} topographical representations of the computed LFP rate mean (b). Quantification of the mean LFP, SWR, and MUA rates between APP^{NL} and APP^{NL-G-F} (c), based on recordings from representative slices with n=3,083 (APP^{NL}) and 3,067 (APP^{NL-G-F}) total firing electrodes. Box-and-whisker plots show the interquartile range (25th–75th percentiles) with whiskers extending up to 1.5 times the IQR. Some items are created with BioRender.

III. Results and Discussion

A. Network Dysfunction in AD Models

To assess hippocampal circuit dysfunction in Alzheimer's disease, we compared local field potential (LFP), sharp-wave ripple (SWR), and multi-unit activity (MUA) patterns between APP^{NL} and APP^{NL-G-F} mouse models. Quantitative analysis revealed that while LFP event rates remained similar between genotypes, APP^{NL-G-F} mice exhibited a significant reduction in SWR and MUA rates (Fig. 1c). Further spectral analysis indicated a loss of high-frequency oscillatory power, with pronounced deficits in SWRs, which are critical for memory consolidation (Fig. 3, a and b, *no saffron condition*). These findings align with human AD studies, where hippocampal-cortical decoupling is associated with cognitive impairment [18]. Additionally, SWR events in APP^{NL-G-F} slices showed shorter durations and decreased spatial distribution, particularly in CA3 and CA1 (Fig. 2d; Fig. 4, a and c, *no saffron condition*), suggesting weakened recurrent excitation within hippocampal subcircuits.

These findings highlight the vulnerability of high-frequency oscillations to advanced AD pathology, where synaptic and structural integrity are severely compromised, leading to disruptions in the coordinated activity required for memory consolidation and cognitive functions. Differences in Aβ and tau pathology between the APP^{NL} and APP^{NL-G-F} models may explain the greater impairment observed in APP^{NL-G-F} mice, as tau-related dysfunction exacerbates both neuronal excitability deficits and interneuron-mediated inhibition, resulting in more pronounced ripple impairments and network desynchronization [1], [3], [13], [14].

B. Saffron Modulation of Circuit Activity

To examine whether saffron could modulate network dysfunction, we applied increasing concentrations of saffron (0, 25, 50, and 75 µg/mL) and quantified changes in circuit activity (Fig. 2, a-c). Saffron induced a dose-dependent recovery of SWR and MUA activity, with significant effects observed at 25 µg/mL [12]. In APP^{NL-G-F} slices, both SWR rates (Fig. 2b) and MUA spiking rates (Fig. 2c) significantly increased, recovering to their respective APP^{NL} baseline responses, particularly in CA3 and CA1 HC subregions (Fig. 2d). Interestingly, higher doses (50–75 µg/mL) did not significantly enhance responses further.

This dose-dependent increase in SWR activity suggests that saffron progressively modulates network disruptions and enhances CA3-CA1 communication, while APP^{NL} HC circuitry likely reaches a functional ceiling due to its more preserved network integrity [13], [14]. Interestingly, APP^{NL} slices showed minimal changes in network activity, suggesting that saffron primarily exerts effects in pathologically impaired circuits rather than enhancing baseline oscillations. This specificity supports its role in network restoration rather than general excitation.

C. Dose-Dependent Response and Network Recovery

To characterize the temporal signature differences and highlight frequency-specific contributions to the network recovery between APP^{NL} and APP^{NL-G-F}, successive temporal traces comparison and spectral analysis were performed between no saffron and 25 µg/mL application. This revealed modulated recovery in the timing and frequency of SWR activity and recovery of high-frequency oscillatory power in the APP^{NL-G-F} HC circuit (Fig. 3, a and b). To further quantify saffron's effects, we performed event-based analyses. The number of active electrodes detecting SWR events increased 2.75-fold in APP^{NL-G-F} slices after 25 µg/mL application, indicating broader network engagement (Fig. 4a). SWR event rates also increased proportionally (Fig. 4b), while event durations became comparable to APP^{NL} values (Fig. 4c).

These findings suggest that saffron restores functional aspects of hippocampal oscillatory dynamics by improving synaptic coordination and circuit integrity. Interestingly, SWR recovery followed a non-linear dose-response relationship, as quantified by the EC50 value (~25 µg/mL, Fig. 2). At higher concentrations, SWR enhancement plateaued, which may reflect a ceiling effect in network responsiveness. This suggests that saffron facilitates synaptic restoration up to a certain threshold, beyond which additional effects are limited by the underlying pathology.

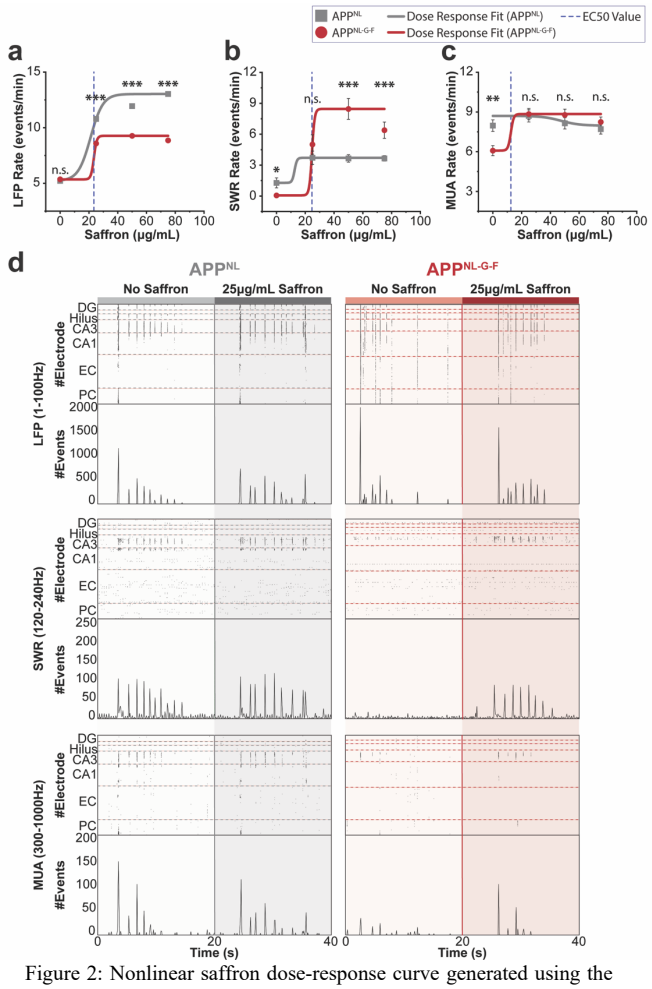

Figure 2: Nonlinear saffron dose-response curve generated using the Levenberg-Marquardt iteration algorithm indicating an EC_{50} value of ~25 µg/mL across LFP (a), SWR (b). and MUA (c) frequency bands. Raster plots comparing 0 µg/mL and 25 µg/mL saffron doses in APP^{NL} and APP^{NL-G-F} HC circuits for each frequency band (d). Interval plots represent the mean ± SEM.

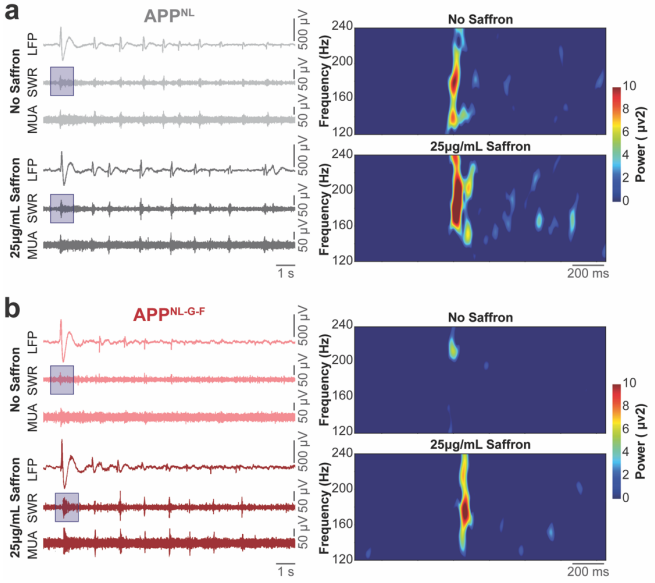

Figure 3: 10 s of temporal signal traces of band-pass filtered LFP (1–100 Hz), SWR (120–240 Hz), and MUA (300–1000 Hz) from the hippocampal CA3 subregion comparing 0 µg/mL and 25 µg/mL saffron doses in APP^{NL} (a) and APP^{NL-G-F} (b) HC circuits. Pseudo-color spectrogram insets illustrate SWR frequency-time dynamics.

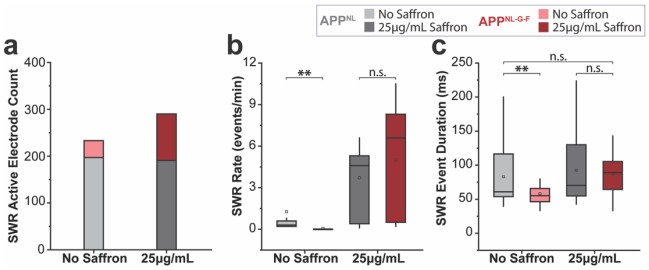

Figure 4: Quantification of SWR active electrode count (a), mean SWR rate (b), and mean SWR event duration (c) comparing 0 µg/mL and 25 µg/mL saffron doses in APP^{NL} and APP^{NL-G-F} HC circuits. Box-and-whisker plots show the interquartile range (25th–75th percentiles) with whiskers extending up to 1.5 times the IQR.

IV. Conclusion

This study establishes HD-MEA as a powerful platform for characterizing hippocampal circuit dysfunction in Alzheimer's disease (AD). Our findings reveal significant disruptions in SWR and MUA in the APP^{NL-G-F} model, indicating that large-scale network impairments are a hallmark of AD progression. These results reinforce the need to move beyond molecular pathology and incorporate network-wide biomarkers for a more comprehensive understanding of neurodegenerative diseases.

Saffron application showed dose-dependent modulation of network activity, particularly in the more impaired APP^{NL-G-F} model, suggesting a potential role in circuit-level regulation. However, the saturation of effects at higher doses highlights the complexity of modulating network activity and the need for further mechanistic investigations. Future studies should explore whether such modulation translates to long-term functional recovery and cognitive improvements *in vivo*. As a proof-of-concept study, these findings establish a foundation for future large-scale investigations aimed at elucidating the precise dose-dependent effects and underlying mechanisms of saffron's neuromodulatory actions.

Beyond AD, this study demonstrates the broader applicability of the HD-MEA platform in investigating circuit dysfunction across neurological and psychiatric disorders. Large-scale electrophysiology can be used to probe network abnormalities in conditions such as epilepsy, schizophrenia, and traumatic brain injury, where disrupted oscillatory dynamics play a central role. By integrating this method with behavioral paradigms, imaging, and molecular analyses, future research can establish stronger links between circuit dysfunction and disease mechanisms, paving the way for network-based interventions and precision therapeutics.

Acknowledgment

We would like to acknowledge the platform for behavioral animal testing at the DZNE-Dresden for their support.

References

[1] G. Buzsáki, "Large-scale recording of neuronal ensembles," *Nat Neurosci*, vol. 7, no. 5, pp. 446–451, 2004.

[2] A. Draguhn and G. Buzsáki, "Neuronal Oscillations in Cortical Networks," *Science (1979)*, vol. 304, no. June, pp. 1926–1930, 2004.

[3] G. Buzsáki, "Hippocampal sharp wave-ripple: A cognitive biomarker for episodic memory and planning," *Hippocampus*, vol. 25, no. 10, pp. 1073–1188, Oct. 2015.

[4] J. J. Palop and L. Mucke, "Network abnormalities and interneuron dysfunction in Alzheimer disease," *Nat Rev Neurosci*, vol. 17, no. 12, pp. 777–792, 2016.

[5] J. J. Palop, J. Chin, and L. Mucke, "A network dysfunction perspective on neurodegenerative diseases," *Nature*, vol. 443, pp. 768–773, 2006.

[6] S. F. Grieco, T. C. Holmes, and X. Xu, "Probing neural circuit mechanisms in Alzheimer's disease using novel technologies," 2023, *Springer Nature*.

[7] Z. Breijyeh and R. Karaman, "Comprehensive Review on Alzheimer's Disease: Causes and Treatment," Dec. 01, 2020, *MDPI*.

[8] A. Serrano-Pozo, M. P. Frosch, E. Masliah, and B. T. Hyman, "Neuropathological alterations in Alzheimer disease," *Cold Spring Harb Perspect Med*, vol. 1, no. 1, Sep. 2011.

[9] B. A. Emery, S. Khanzada, X. Hu, D. Klütsch, and H. Amin, "Recording and Analyzing Multimodal Large-Scale Neuronal Ensemble Dynamics on CMOS-Integrated High-Density Microelectrode Array," *Journal of Visualized Experiments*, no. 205, Mar. 2024.

[10] B. A. Emery, X. Hu, S. Khanzada, G. Kempermann, and H. Amin, "High-resolution CMOS-based biosensor for assessing hippocampal circuit dynamics in experience-dependent plasticity," *Biosens Bioelectron*, vol. 237, Oct. 2023.

[11] X. Hu, S. Khanzada, D. Klütsch, F. Calegari, and H. Amin, "Implementation of biohybrid olfactory bulb on a high-density CMOS-chip to reveal large-scale spatiotemporal circuit information," *Biosens Bioelectron*, vol. 198, Feb. 2022.

[12] H. Amin, T. Nieus, D. Lonardoni, A. Maccione, and L. Berdondini, "High-resolution bioelectrical imaging of Aβ-induced network dysfunction on CMOS-MEAs for neurotoxicity and rescue studies," *Sci Rep*, vol. 7, no. 1, pp. 1–13, 2017.

[13] A. Latif-Hernandez *et al.*, "The two faces of synaptic failure in AppNL-G-F knock-in mice," *Alzheimers Res Ther*, vol. 12, no. 1, p. 100, Dec. 2020.

[14] T. Saito *et al.*, "Single App knock-in mouse models of Alzheimer's disease," *Nat Neurosci*, vol. 17, no. 5, pp. 661–663, May 2014.

[15] M. A. Maggi, S. Bisti, and C. Picco, "Saffron: Chemical Composition and Neuroprotective Activity," *Molecules*, vol. 25, no. 23, p. 5618, Nov. 2020.

[16] M. Spinelli, A. Biancolillo, G. Battaglia, M. Foschi, A. Amoresano, and M. A. Maggi, "Saffron Characterization by a Multidisciplinary Approach," *Molecules*, vol. 28, no. 1, Jan. 2023.

[17] X. Hu, B. A. Emery, S. Khanzada, and H. Amin, "DENOISING: Dynamic enhancement and noise overcoming in multimodal neural observations via high-density CMOS-based biosensors," *Front Bioeng Biotechnol*, vol. 12, Sep. 2024.

[18] B. A. Mander *et al.*, "β-amyloid disrupts human NREM slow waves and related hippocampus-dependent memory consolidation," *Nat Neurosci*, vol. 18, no. 7, pp. 1051–1057, Jul. 2015.